

# Fluctuations of the chiral condensate and quasi-particle spectra near phase transition

<sup>a</sup>Yukio Nemoto, <sup>b</sup>Masakiyo Kitazawa and <sup>c</sup>Teiji Kunihiro

<sup>a</sup>*Department of Physics, Nagoya University, Nagoya 464-8602, Japan*

<sup>b</sup>*Department of Physics, Osaka University, Toyonaka, Osaka 560-0043, Japan*

<sup>c</sup>*Yukawa Institute for Theoretical Physics, Kyoto University, Kyoto 606-8502, Japan*

## Abstract

We investigate the quark spectrum near but above the critical temperature of the chiral transition, taking into account the precursory soft modes. It is found that there appear novel excitation spectra of quasi-quarks and quasi-antiquarks with a three-peak structure. By a detailed analysis on the formation of the three-peak structure using Yukawa models, it is shown that the new quark spectra originate from the mixing between a quark (anti-quark) and an antiquark hole (quark hole) caused by a resonant scattering of the quasi-quark with the soft modes which have a small but finite excitation energy with a small width near the critical temperature.

## 1 Introduction

Recently, it is believed that the quark-gluon plasma (QGP) just above the chiral and deconfinement phase transitions is an unexpectedly strongly interacting system, which is mainly based on the facts that the created matter at RHIC behaves like a perfect fluid [1] and that some mesonic bound states of heavy quarks can survive above the critical temperature ( $T_c$ ) from Lattice QCD studies [2]. Because the fundamental degrees of freedom in QGP are quarks and gluons, it is also important to study their properties in such a strongly interacting system. Here, we investigate the quark spectrum just above  $T_c$  of the chiral transition, focusing on the precursory soft modes. It is known that the soft modes exist over a wide range of temperature above  $T_c$  owing to a strong coupling nature between quarks [3]. In this work, we show that they affect the quark spectrum significantly in a region just above  $T_c$ . In particular, it is shown that the quark spectrum form three-peaks at low energy and low momentum region near  $T_c$  [4].

In Sec.2, using a chiral effective model, we show that the quark spectrum near  $T_c$  forms the three-peak structure owing to a coupling with the soft modes. Such a three-peak structure is seen more clearly if the soft modes are replaced by an elementary massive boson [5]. In Sec.3, a detailed analysis on the quark spectrum is given using Yukawa models with a massless quark and a massive scalar (pseudoscalar) or vector (axialvector) boson. We elucidate the mechanism of the formation of the three-peak structure through which the new quark collective excitations are realized in terms of the Landau damping of a quark (an antiquark) induced by scattering with the thermally excited boson, which gives rise to mixing

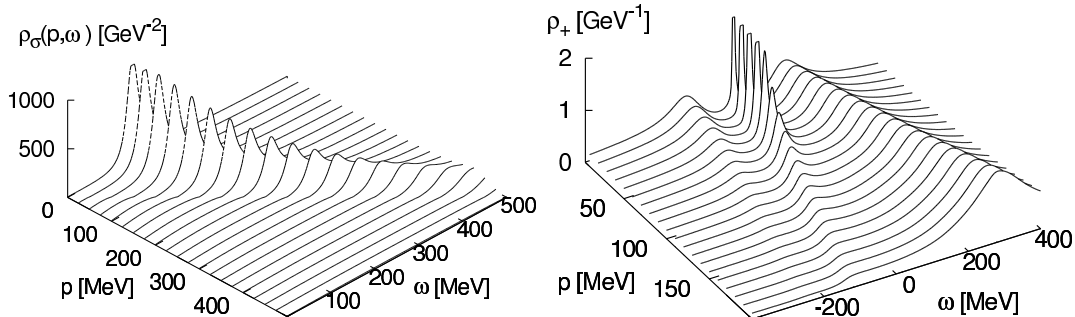


Figure 1: The spectral function  $\rho_\sigma \equiv \rho$  in the quark-antiquark channel (left) and the quasi-quark spectral function  $\rho_+$  (right) for  $\mu = 0$  and  $\varepsilon \equiv (T - T_c)/T_c = 0.1$ .

and hence a level repulsion between a quark (antiquark) and an antiquark hole (quark hole). Brief summary and concluding remarks are given in Sec.4.

## 2 Quark spectrum near chiral transition

To describe the chiral transition and the fluctuations, we first employ the two-flavor Nambu–Jona-Lasinio model in the chiral limit

$$\mathcal{L} = \bar{\psi}i\partial\psi + G_S[(\bar{\psi}\psi)^2 + (\bar{\psi}i\gamma_5\vec{\tau}\psi)^2], \quad (1)$$

with the coupling constant  $G_S = 5.5 \text{ GeV}^{-2}$  and the three dimensional cutoff  $\Lambda = 631 \text{ MeV}$  taken from Ref. [3]. This model gives a second order phase transition at  $T_c = 193.5 \text{ MeV}$  for vanishing quark chemical potential.

The fluctuations of the chiral condensate are described by the quark-antiquark Green function in the random phase approximation,

$$\mathcal{D}(\mathbf{p}, \nu_n) = -\frac{1}{1/(2G_S) + \mathcal{Q}(\mathbf{p}, \nu_n)}, \quad (2)$$

where  $\nu_n = 2\pi nT$  is the Matsubara frequency for bosons and  $\mathcal{Q}(\mathbf{p}, \nu_n)$  is the undressed quark-antiquark polarization function at one-loop. To evaluate strengths of the fluctuations, we employ the spectral function,  $\rho$ , given by

$$\rho(\mathbf{p}, \omega) = -\frac{1}{\pi} \text{Im} \mathcal{D}(\mathbf{p}, \nu_n)|_{i\nu_n = i\omega + i\eta}. \quad (3)$$

We show  $\rho(\mathbf{p}, \omega)$  near  $T_c$  in the left panel of Fig. 1. One can see that there appear pronounced peaks which denote the precursory soft modes [3]. The peak positions of the modes are approximately expressed as  $\omega \simeq \pm\sqrt{m_\sigma^*(T)^2 + \mathbf{p}^2}$ . A  $T$ -dependent ‘mass’  $m_\sigma^*(T)$  becomes smaller as  $T$  approaches  $T_c$ , which means the softening at  $T_c$ .

The effect of the soft modes on the quark spectrum is incorporated in the quark self-energy in a non-selfconsistent way,

$$\tilde{\Sigma}(\mathbf{p}, \omega_n) = -4T \sum_m \int \frac{d^3q}{(2\pi)^3} \mathcal{D}(\mathbf{p} - \mathbf{q}, \omega_n - \omega_m) \mathcal{G}_0(\mathbf{q}, \omega_m), \quad (4)$$

where  $\mathcal{G}_0(\mathbf{q}, \omega_m)$  is the free quark propagator with  $\omega_n = (2n + 1)\pi T$  being the Matsubara frequency for fermions. The quasi-quark and quasi-antiquark spectral functions,  $\rho_{\pm}(\mathbf{p}, \omega)$ , are obtained from the retarded self-energies,  $\Sigma_{\pm}^R(\mathbf{p}, \omega) = (1/2)\text{Tr}[\Sigma^R \gamma^0 \Lambda_{\pm}]$ , respectively, i.e.

$$\rho_{\pm}(\mathbf{p}, \omega) = -\frac{1}{\pi} \text{Im}[\omega \mp |\mathbf{p}| - \Sigma_{\pm}^R(\mathbf{p}, \omega)]^{-1}, \quad (5)$$

with the analytic continuation  $\Sigma^R(\mathbf{p}, \omega) = \tilde{\Sigma}(\mathbf{p}, \omega_n)|_{i\omega_n = \omega + i\eta}$  and the projection operators  $\Lambda_{\pm} = (1 \pm \gamma^0 \boldsymbol{\gamma} \cdot \mathbf{p}/|\mathbf{p}|)/2$ .

The quasi-quark spectral function  $\rho_+$  for  $\mu = 0$  MeV and  $\varepsilon \equiv (T - T_c)/T_c = 0.1$  is plotted in the right panel of Fig. 1. We see a clear three-peak structure at low momentum, which exists even at  $\varepsilon = 0.2$  [4]. Although not shown in the figure, the quasi-antiquark spectrum,  $\rho_-$ , has also a three-peak structure for a relation,  $\rho_-(\mathbf{p}, \omega) = \rho_+(\mathbf{p}, -\omega)$ . The mechanism of the appearance of the three-peak structure in  $\rho_+$  is as follows: The imaginary part of  $\Sigma_+^R(\mathbf{0}, \omega)$  has two peaks at nonzero values of  $\omega$ , which means that there exist two large damping modes of the quasi-quark there. From a kinematical consideration which is explained in detail in the following section, we see that one is a collision of a thermally excited antiquark and the quasi-quark creating the soft mode, and the other is a collision of the quasi-quark and the soft mode creating an on-shell quark. Both the processes are interpreted as a Landau damping of the quasi-quark. The point is that the quasi-quark is a mixed state between quarks and ‘antiquark-holes’ which are annihilation of thermally excited antiquarks and have the positive quark number. Then, these damping modes cause a mixing between quarks and antiquark-holes. This mixing mechanism can be described in terms of the resonant scattering as in the case of the color superconductivity [6], although a crucial difference arises owing to the different nature of the soft modes. We can show that a coupling with the soft mode with a *nonzero mass*  $m_{\sigma}^*(T)$  is essential for the appearance of the three-peak structure in the quark spectrum, as will be explained below in Yukawa models.

### 3 Quark spectrum in Yukawa models

As mentioned above, the soft modes of the chiral transition have the character of a well-defined elementary boson with a mass  $m_{\sigma}^*(T)$  and a small width near  $T_c$ . Thus it is seen that a coupling with an elementary massive boson is favorable for the three-peak structure of the quark spectrum. In this section, we show that a system composed of a massless quark and a massive boson, as described by Yukawa models, exhibits the three-peak structure in the quark spectral function [5].

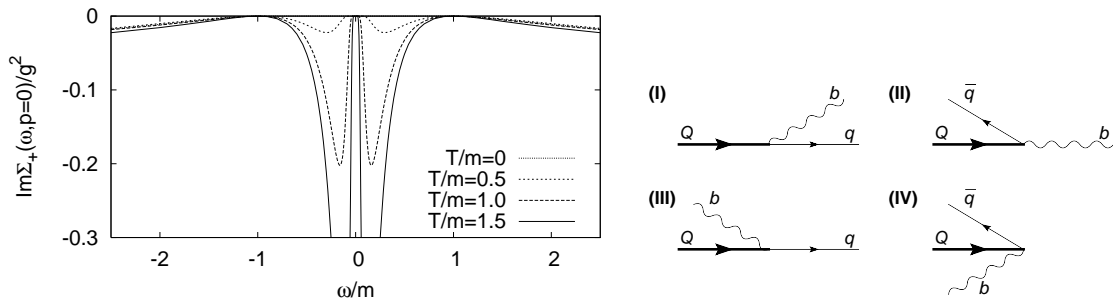


Figure 2:  $\text{Im}\Sigma_{\pm}(\mathbf{p} = 0, \omega)$  for several temperatures (left) and the kinetic processes in  $\text{Im}\Sigma_{\pm}(\mathbf{p}, \omega)$ .  $Q$  represents the quasi-quark,  $q$  on-shell free quarks and  $b$  the on-shell scalar boson. The incident on-shell particles are thermally excited particles.

### 3.1 Scalar (pseudoscalar) boson

We first investigate the spectrum of a massless quark coupled with a massive scalar (pseudoscalar) boson at finite  $T$  in a Yukawa model:

$$\mathcal{L} = \bar{\psi}(i\cancel{\partial} - g\phi)\psi + \frac{1}{2}(\partial_{\mu}\phi\partial^{\mu}\phi - m^2\phi^2). \quad (6)$$

$g$  is the coupling constant and  $m$  is the boson mass.

The quark self-energy in the imaginary time formalism at the one-loop order is expressed as

$$\tilde{\Sigma}(\mathbf{p}, i\omega_m) = -g^2 T \sum_n \int \frac{d^3\mathbf{k}}{(2\pi)^3} \mathcal{G}_0(\mathbf{k}, i\omega_n) \mathcal{D}(\mathbf{p} - \mathbf{k}, i\omega_m - i\omega_n) \quad (7)$$

where  $\mathcal{G}_0(\mathbf{k}, i\omega_n) = [i\omega_n\gamma^0 - \mathbf{k} \cdot \boldsymbol{\gamma}]^{-1}$  and  $\mathcal{D}(\mathbf{k}, i\nu_n) = [(i\nu_n)^2 - \mathbf{k}^2 - m^2]^{-1}$  are the Matsubara Green functions for the free quark and scalar boson, respectively, and  $i\omega_n = (2n+1)\pi T$  and  $i\nu_n = 2n\pi T$  are the Matsubara frequencies for the fermion and boson, respectively.

For the coupling with a pseudoscalar boson, a factor  $i\gamma_5$  is added in both sides of  $\mathcal{G}_0$  in eq. (7). Such a factor is, however, canceled out because it anti-commutes with  $\mathcal{G}_0$  and thus the self-energy becomes the same form as eq (7). Therefore, the following results and discussion in this section hold also for the coupling with a pseudoscalar boson.

After the Matsubara summation and the analytic continuation, the retarded self-energy is obtained. In the left panel of Fig. 2, we show  $\text{Im}\Sigma_{+}(\mathbf{p} = 0, \omega)/g^2$ , which is independent of  $g$ . We see that it vanishes at  $\omega = 0, \pm m$ , irrespective of  $T$ . The vanishing decay rate at  $\omega = \pm m$  is owing to the suppression of the phase space; the energy-momentum conservation requires the zero momentum of the on-shell (anti)quark for each process at  $\omega = \pm m$ . Around  $\omega = 0$ , on the other hand, the distribution functions suppress the decay rate, because the on-shell energies of the boson and the quark go to infinity as  $\omega \rightarrow 0$ .

At finite  $T$ , the Landau damping, the processes (II) and (III) in the right panel of Fig. 2, comes to play and  $\text{Im}\Sigma_{+}(\mathbf{0}, \omega)$  have supports in the regions  $-1 < \omega/m < 0$  for (II) and

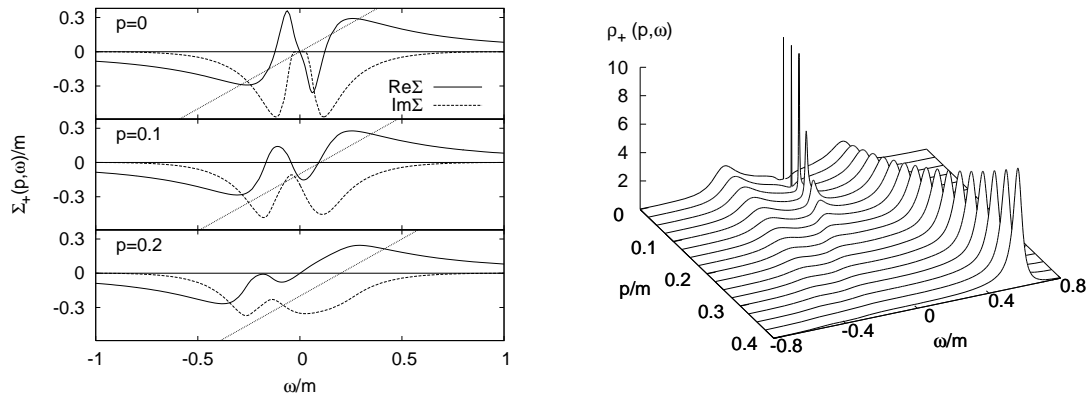


Figure 3: The quark self-energy  $\Sigma_+(\mathbf{p}, \omega)$  (left) and the quark spectral function  $\rho_+(\mathbf{p}, \omega)$  (right) for  $T/m = 1.4$ . The dotted straight line in the left panel denotes  $\omega - |\mathbf{p}|$ .

$0 < \omega/m < 1$  for (III). These two peaks in these regions grow rapidly as  $T$  is raised, and around  $T \simeq m$ , the Landau damping is dominant.

The corresponding quark spectral function around for  $T/m = 1.4$  in the right panel of Fig. 3 shows a peculiar behavior. There appear broad peaks both in the positive- and negative-energy regions as well as the narrow peak around the origin for lower momenta: Thus the spectral function in the low-momentum region has *three peaks*. To understand the behavior of  $\rho_+(\mathbf{p}, \omega)$ , we show  $\Sigma_+(\mathbf{p}, \omega)$  for  $T/m = 1.4$  in the left panel of Fig. 3. We see that the oscillatory change of the real part around  $\omega \sim 0$  is seen, reflecting the peaks in the imaginary part. It is noted that in general, a sharp peak in the spectral function can be formed at  $(\omega, \mathbf{p})$  if the quasi-dispersion relation,  $\omega - |\mathbf{p}| - \text{Re}\Sigma_+ = 0$ , and a relation  $\text{Im}\Sigma_+/\text{Re}\Sigma_+ \ll 1$  are hold. In order to find out the quasi-dispersion relation from Fig. 3, we draw the line  $\omega - |\mathbf{p}|$ . For vanishing momenta, we see that there appear five crossing points of  $\text{Re}\Sigma_+$  and  $\omega - |\mathbf{p}|$ . The crossing points with the second and fourth largest  $\omega$ , however, are located at the energies of the peak of  $|\text{Im}\Sigma_+(\mathbf{p}, \omega)|$  and hence the spectral function does not form a peak there. The other three crossing points correspond to the three peaks in the spectral function. For large momenta, the number of the crossing points decreases and eventually only one crossing point remains.

At higher temperature, the strength of the peak around the origin is getting weaker, and eventually there remain the other two peaks which correspond to the normal quasi-quark and the plasmino in the HTL approximation.

To understand the physical mechanism responsible for the three-peak structure of  $\rho_+(\mathbf{p}, \omega)$ , we first recall that there develop two peaks in  $\text{Im}\Sigma_+$  which correspond to the decay processes (II) and (III). The process (II) is the annihilation process of the incoming quark  $Q$  and the thermally excited antiquark into a boson in the thermal bath,  $Q + \bar{q} \rightarrow b$ , and its inverse process. Two remarks are in order here. First, the disappearance of an anti-quark implies the

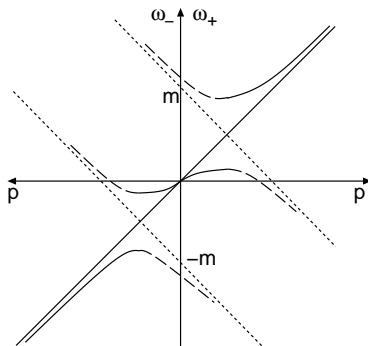


Figure 4: Typical peak position of the spectral functions in the case of level mixing away from the origin. The long dashed curves show that the strength of the spectrum is becoming weaker. The solid line represents the free quark and antiquark dispersion relations, and the dotted line the antiquark hole and quark hole dispersion relations. Level repulsion takes place at the intersection point of these two lines.

creation of a ‘hole’ in the thermally excited anti-quark distribution[7]. Second, the creation of bosons in a thermal bath is enhanced in comparison with the case in vacuum by a statistical factor of  $1 + n$ , which becomes large when  $T$  is comparable to  $m$ . Thus, we see that the process (II) causes a virtual mixing between the quark and ‘anti-quark hole’ states and as a result, the mixing is enhanced when  $T/m \sim 1$ .

The process (III) is another decay process of a quasi-quark state  $Q$ , which is now understood to be a mixed state of quarks and antiquark-holes, into an on-shell quark via a collision with a thermally excited boson:  $Q + b \rightarrow q$  and its inverse process. These processes again give rise to a mixing of a quasi-quark and an anti-quark hole state.

The mechanism for the mixing of the quark and hole state can also be characterized as a *resonant scattering* [6, 8], which was originally introduced to understand the non-Fermi liquid behavior of fermions just above the critical temperature of the superconducting. In fact, we have seen that the process (II) includes a scattering process of the quark by a massive boson, thus creating a hole state in the thermally distributed anti-quark states:  $Q \rightarrow \bar{q}_h + b$ . Such a process is called resonant scattering[6, 8]. Note that the most probable process for finite  $T$  involves the lowest energy state of the boson, i.e., a rest boson with a energy  $m$ . The energy conservation law in the most probable case for the above process is  $\omega_Q(\mathbf{p}) + \omega_{\bar{q}}(-\mathbf{p}) = m$ , or equivalently,  $\omega_Q(\mathbf{p}) = m - \omega_{\bar{q}}(-\mathbf{p})$ . This equation actually represents the energy-momentum relation for the particles involved in the state mixing. Thus we see that the physical energy spectrum is obtained as a result of the level repulsion between the energies  $\omega_q(\mathbf{p}) = |\mathbf{p}|$  and  $m - \omega_{\bar{q}}(-\mathbf{p}) = m - |\mathbf{p}|$  in the perturbative picture. This situation is schematically depicted in the upper right part of Fig. 4.

Similarly, the process (III) includes the process  $q \rightarrow Q + b$ , and the energy-momentum conservation law for this process for the most probable case is  $-\omega_q(\mathbf{p}) = -m + \omega_Q(\mathbf{p})$ . Thus,

the physical energy spectrum is obtained as a result of the level repulsion between the energies  $-|\mathbf{p}|$  and  $-m + |\mathbf{p}|$ . This situation is also depicted in the lower-right part in Fig. 4.

We thus find that at temperatures satisfying  $T/m \sim 1$ , owing to the finite boson mass, the level repulsions occur far from the origin and two gap-like structures in the quark spectrum are formed at positive and negative energies, as shown in Fig. 4.

At the high temperature limit,  $T \gg m$ , or  $m/T \sim 0$ , the effect of the boson mass can be ignored, and the resonant scattering occurs only once at the origin ( $\omega = |\mathbf{p}| = 0$ ), since the energy levels which are to be repelled cross only there. Then the quark spectrum has two peaks in the positive and negative energy region, which is realized in the HTL approximation.

It was shown in the previous section that the quark spectral function possesses a three-peak structure near  $T_c$  of the chiral transition when the chiral soft mode is incorporated into the quark self-energy. Recall that the soft modes behave like a massive elementary boson with a mass  $m_\sigma^*(T)$  as  $T$  approaches  $T_c$ , i.e.  $\omega \sim \sqrt{\mathbf{p}^2 + m_\sigma^*(T)^2}$ , and hence the quark spectra in such a case are essentially the same as that treated in this section. We also note that as  $T$  is lowered toward  $T_c$ ,  $m_\sigma^*(T)$  tends to vanish, and hence the ratio  $T/m_\sigma^*(T)$  becomes large. Thus the quark spectrum approaches that in the  $T/m \rightarrow \infty$  limit of the Yukawa model.

### 3.2 Vector (axialvector) boson

In this subsection, we investigate the quark spectrum using a Yukawa model with a massive vector (axial-vector) boson and show that the three-peak structure of the quark spectral function is obtained.

We start from the following Lagrangian, composed of a massless quark  $\psi$  and vector boson field  $V_\mu$ :

$$\mathcal{L} = \bar{\psi}(i\cancel{\partial} - ig\gamma^\mu V_\mu)\psi - \frac{1}{4}F_{\mu\nu}F^{\mu\nu} + \frac{1}{2}m^2V_\mu V^\mu, \quad (8)$$

with the field strength  $F_{\mu\nu} = \partial_\mu V_\nu - \partial_\nu V_\mu$ .

At one-loop order, the quark self-energy in the imaginary time formalism is given by

$$\tilde{\Sigma}(\mathbf{p}, i\omega_m) = -g^2 T \sum_n \int \frac{d^3\mathbf{k}}{(2\pi)^3} \gamma^\mu \mathcal{G}_0(\mathbf{k}, i\omega_n) \gamma^\nu \mathcal{D}_{\mu\nu}(\mathbf{p} - \mathbf{k}, i\omega_m - i\omega_n), \quad (9)$$

with the Matsubara propagator for the massive vector boson,

$$\mathcal{D}_{\mu\nu}(i\nu_n, \mathbf{p}) = -\frac{g_{\mu\nu} - \tilde{p}_\mu \tilde{p}_\nu / m^2}{\tilde{p}_\mu \tilde{p}^\mu - m^2}, \quad (10)$$

where  $\tilde{p}_\mu = (i\nu_n, \mathbf{p})$ .

For coupling with an axial-vector boson, as the self-energy has the same form as Eq. (9), the following results hold also.

In the left panel of Fig. 5, we plot  $\text{Im}\Sigma_+(\mathbf{p} = 0, \omega)$  at  $T/m = 0, 0.5, 1$  and  $1.5$ . We fix the coupling constant at  $g = 1$ . The qualitative features of both parts for  $|\omega|/m < 1$  are quite similar to those in the left panel of Fig. 2: There are two clear peaks in  $\text{Im}\Sigma_+$  for  $|\omega|/m < 1$

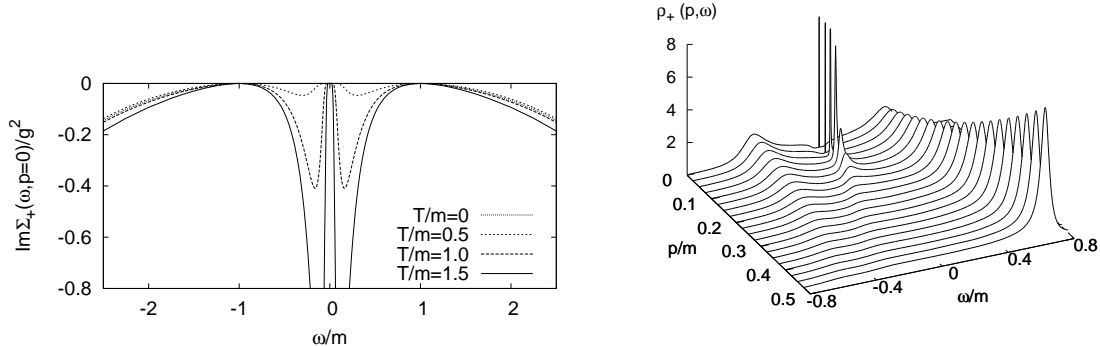


Figure 5:  $\text{Im}\Sigma_+(\mathbf{p} = 0, \omega)$  for several temperatures (left) and the quark spectral function  $\rho_+(\mathbf{p}, \omega)$  for  $T/m = 1.2$  (right).

and they grow rapidly as  $T$  increases. For  $|\omega|/m > 1$ , it is seen that  $|\text{Im}\Sigma_+(\mathbf{p} = 0, \omega)|$  grows more rapidly than in the Yukawa model with the scalar boson shown in Fig. 2.

In the right panel of Fig. 5, we plot the quark spectral function for  $T/m = 1.2$ . It is seen that there appears a three-peak structure, as found in the previous subsection. This is quite natural, and it would be expected from the behavior of the self-energy. A clear three-peak structure is formed at lower values of  $T$  than in the scalar boson case, which comes from the difference of the matrix elements between the scalar and vector boson.

## 4 Summary and concluding remarks

We have investigated the quark spectrum near but above the critical temperature of the chiral phase transition taking the effect of the fluctuations of the chiral order parameter into account. We have shown that for  $\varepsilon \equiv (T - T_c)/T_c \lesssim 0.2$  the quark spectrum has a three-peak structure at low frequency and low momentum. The mechanism of the formation of the three-peak structure is based on the fact that the soft modes which are composite system of quark-antiquarks acquire the character of the well-defined elementary bosonic excitation when  $T$  is close to  $T_c$ .

Then, we have elucidated the essential mechanism of the formation of the three-peak structure quantitatively in Yukawa models composed of a massless quark and a massive boson with a mass  $m$  at finite  $T$ , in which the mass of the boson field is varied by hand. We have found that the quark spectral function at low frequency and low momentum has a three-peak structure at intermediate values of  $T$ , i.e. for  $T/m \sim 1$ , which is independent of the species of the massive boson. Among them, the two peaks have finite thermal masses and approach the normal quasi-quark and plasmino excitations in the HTL approximation in the high  $T$  limit, while the strength of the other peak around the origin becomes weaker and disappears in this limit.



We have discussed the fact that the three-peak structure originates from the Landau damping, that is, the scattering processes of a quark and an antiquark hole of a thermally excited antiquark, and of an antiquark and a quark hole of a thermally excited quark. They cause the formation of energy gaps in the quark spectrum, owing to the level mixing between the quark (antiquark) and the hole of the thermally excited antiquarks (quarks). This leads to a level repulsion or gap in the resultant physical spectrum. These mixings can be understood in terms of the resonant scattering [6, 8] of the quasi-quarks off the bosons. In particular, owing to the mass of the boson, the level repulsion due to the resonant scattering occurs *twice* at different points in the energy-momentum plane, leading to the three-peak structure of the spectral function. This contrasts with the case of the quark spectrum coupled to a massless boson, such as a gauge boson, in which the resonant scattering occurs only at the origin in the energy-momentum plane and then leads to only two peaks, as in the spectrum in the HTL approximation [7].

The soft modes for the chiral transition behave like a massive elementary boson with a mass  $m_\sigma^*(T)$  as  $T$  approaches  $T_c$ , i.e.  $\omega \sim \sqrt{\mathbf{p}^2 + m_\sigma^*(T)^2}$ , and hence the quark spectra in such a case are essentially the same as that treated in the Yukawa models. We also note that as  $T$  is lowered toward  $T_c$ ,  $m_\sigma^*(T)$  tends to vanish, and hence the ratio  $T/m_\sigma^*(T)$  becomes large. Thus the quark spectrum approaches that in the  $T/m \rightarrow \infty$  limit of the Yukawa models.

In this work, we have considered only massless quarks. A finite quark mass should affect the formation of the three-peak structure in the quark spectral function. Thus, the incorporation of the quark mass effect is important for describing the chiral transition precisely, because the order of the transition, and hence, the quark spectrum near the critical point are sensitive to the quark mass. A finite quark mass also leads to a difference between the scalar (vector) and pseudoscalar (axial-vector) boson cases, and may suppress the three-peak structure. Detailed study of such an effect is now under way and will be reported elsewhere[9].

Y.N. is supported by the 21st Century COE Program at Nagoya University and the JSPS Grand-in-Aid for Scientific Research (#18740140). T.K. is supported by a Grand-in-Aid for Scientific Research by Monbu-Kagakusho of Japan (#17540240). This work is supported by the Grand-in-Aid for the 21st Century COE ‘‘Center for Diversity and University in Physics’’ of Kyoto University.

## References

- [1] I. Arsene et al. (BRAHMS Collaboration), Nucl. Phys. A **757** (2005), 1.  
 B. B. Back et al. (PHOBOS Collaboration), Nucl. Phys. A **757** (2005), 28.  
 J. Adams et al. (STAR Collaboration), Nucl. Phys. A **757** (2005), 102.  
 K. Adcox et al. (PHENIX Collaboration), Nucl. Phys. A **757** (2005), 184.
- [2] T. Umeda, R. Katayama, O. Miyamura and H. Matsufuru, Int. J. Mod. Phys. A **16** (2001), 2215.

- M. Asakawa and T. Hatsuda, Phys. Rev. Lett. **92** (2004), 012001.  
S. Datta, F. Karsch, P. Petreczky and I. Wetzorke, Phys. Rev. D **69** (2004), 094507.  
T. Umeda, K. Nomura and H. Matsufuru, Eur. Phys. J. C **39S1** (2005), 9.  
A. Jakovac, P. Petreczky, K. Petrov and A. Velytsky, Phys. Rev. D **75** (2007), 014506 .  
G. Aarts, C. Allton, M. B. Oktay, M. Peardon and J. I. Skullerud, arXiv:0705.2198 [hep-lat].
- [3] T. Hatsuda and T. Kunihiro, Phys. Lett. B **145** (1984), 7; Phys. Rep. **247** (1994), 221.  
[4] M. Kitazawa, T. Kunihiro and Y. Nemoto, Phys. Lett. B **633** (2006), 269; see also hep-ph/0510381.  
[5] M. Kitazawa, T. Kunihiro and Y. Nemoto, Prog. Theor. Phys. **117** 103 (2007), 103.  
[6] M. Kitazawa, T. Kunihiro and Y. Nemoto, Phys. Lett. B **631** (2005), 157.  
[7] H. A. Weldon, Phys. Rev. D **40** (1989), 2410; Physica A **158** (1989), 169; Phys. Rev. D **61** (2000), 036003.  
[8] B. Janko, J. Mary and K. Levin, Phys. Rev. B **56** (1997), R11407.  
[9] M. Kitazawa, T. Kunihiro, K. Mitsutani and Y. Nemoto, in preparation.